Published in final edited form as:
Channels (Austin). 2009 ; 3(4): 249–258.

Comparative effects of H^+ and Ca^{2+} on large-conductance Ca^{2+}- and voltage-gated Slo1 K^+ channels

Shangwei Hou[1,#], **Frank T. Horrigan**[2,#], **Rong Xu**[1], **Stefan H. Heinemann**[3], and **Toshinori Hoshi**[1,*]

[1] Department of Physiology, Richards D100, 3700 Hamilton Walk, University of Pennsylvania, Philadelphia, PA 19104, USA

[2] Molecular Physiology and Biophysics, Baylor College of Medicine, One Baylor Plaza BCM335, Houston, TX 77030

[3] Center for Molecular Biomedicine, Department of Biophysics, Friedrich Schiller University Jena, Hans-Knöll-St. 2, D-07745 Jena, Germany

Summary

Large-conductance Ca^{2+}- and voltage-gated Slo1 BK channels are allosterically activated by depolarization and intracellular ligands such as Ca^{2+}. Of the two high-affinity Ca^{2+} sensors present in the channel, the RCK1 sensor also mediates H^+-dependent activation of the channel. In this study, we examined the comparative mechanisms of the channel activation by Ca^{2+} and H^+. Steady-state macroscopic conductance-voltage measurements as well as single-channel openings at negative voltages where voltage-sensor activation is negligible showed that at respective saturating concentrations Ca^{2+} is more effective in relative stabilization of the open conformation than H^+. Calculations using the Debye-Hückel formulation suggest that small structural changes in the RCK1 sensor, on the order of few angstroms, may accompany the H^+-mediated opening of the channel. While the efficacy of H^+ in activation of the channel is less than that of Ca^{2+}, H^+ more effectively accelerates the activation kinetics when examined at the concentrations equipotent on macroscopic voltage-dependent activation. The RCK1 sensor therefore is capable of transducing the nature of the ligand bound and transmits qualitatively different information to the channel's permeation gate.

Keywords

BK channel; Slo1 channel; Ca^{2+}-dependent K^+ channel; voltage-gated channel; calcium; potassium; proton

Introduction

Slo1 K^+ (BK, KCa1.1, maxiK) channels are well known for their voltage- and Ca^{2+}-dependent activation.[1, 2] While neither depolarization nor Ca^{2+} is required for opening, increases in intracellular Ca^{2+} concentration ($[Ca^{2+}]_i$) shift the voltage dependence of activation to the negative direction so that more channels open at a given voltage, typically following a faster time course.[1, 3] This allosteric gating mechanism, encompassing the channel's gate, voltage sensors and intracellular Ca^{2+} sensors[4–6], allows the channels to participate in numerous

*To whom correspondence should be addressed. hoshi@hoshi.org.
#These authors contributed equally.

Conflicts of interest: The authors declare no conflict of interest.

physiological processes, such as vascular tone control, neuronal firing and neurotransmitter release[7, 8], providing an important functional link between the membrane excitability and the signaling cascade. Dysfunction of Slo1 BK channel complexes is associated with multiple human diseases including epilepsy.[9–11]

One BK channel complex contains four Slo1 pore-forming subunits[12], each of which possesses a transmembrane voltage-sensor domain (VSD)[13] and a large cytoplasmic portion with two recognizable domains, RCK1 (regulator of conductance for K^+) and RCK2.[14, 15] Four sets of RCK1-RCK2 pairs are thought to form an octameric structure termed a "gating ring" immediately cytoplasmic to the four VSDs and the ion conduction-gate module.[16] Opening of the gate to allow K^+ flux is commonly visualized to be accompanied by expansion of the cytoplasmic gating ring[16] facilitated by binding of intracellular ligands, such as Ca^{2+} and Mg^{2+}, to their respective sensor sites. [1, 15, 16] The physical characteristics of the ligand sensor sites, including the high-resolution structures and true binding affinities, are not yet known but the results from mutational studies have identified multiple putative ligand sensors in the RCK1 and RCK2 domains.[1] The RCK1 domain harbors a high-affinity sensor for Ca^{2+} (hereafter referred to as the RCK1 sensor) and a distinct lower-affinity divalent cation sensor, which mediates the Mg^{2+} sensitivity of the channel.[17–19] The RCK2 domain, comprised of the aminoacid residues closer to the distal C-terminus, includes another high-affinity Ca^{2+} sensor termed the Ca^{2+} bowl (hereafter referred to as the Ca^{2+} bowl sensor).[15, 20] While both the RCK1 and Ca^{2+} bowl sensors contribute to Ca^{2+}-dependent activation of Slo1 BK channels, some functional differences between the two sensors have been noted. For example, the two sensors differ in their adequate stimulus/ion selectivity and also in their abilities to regulate the kinetics of gate opening.[19, 21] The RCK1 sensor plays a major role in determining deactivation kinetics at all $[Ca^{2+}]_i$ and activation kinetics at ≥10 μM $[Ca^{2+}]_i$.[19] The Ca^{2+} bowl sensor is particularly important in regulation of activation kinetics at ≤10 μM $[Ca^{2+}]_i$.[19]

Another important difference between the RCK1 sensor and the Ca^{2+} bowl sensor lies in their functional responsiveness to H^+.[22] Lowering intracellular pH (pH_i), as it may occur following ischemia[23, 24], enhances Slo1 currents by shifting the channel's voltage dependence of macroscopic activation to the negative direction with an EC_{50} of 0.35 μM (pH_i = 6.6) and a Hill coefficient of ~2 or greater depending on membrane potential[25], and this pH_i sensitivity requires two His residues, His365 and His394, near or in the RCK1 sensor.[22] The two His residues, His365 and His394, have been postulated to represent the primary H^+ sensors of the Slo1 channel.[26]

The H^+ sensors His365 and His394 may be in a close proximity of Asp367, a critical component in the RCK1 Ca^{2+} sensor[18], suggesting that H^+ may facilitate opening of the channel's gate in a manner similar to that by Ca^{2+}.[26] Consistent with this idea, the Ca^{2+} sensitivity is impaired by double mutations that disrupt the pH_i sensitivity of the Slo1 channel, H365R:H394R and H365A:H394A and the mutation D367A, which interferes with full Ca^{2+} sensitivity[18], also disrupts pH_i sensitivity.[26] The results of these mutagenesis studies therefore suggest that the RCK1 sensor transduces changes in concentrations of both H^+ and Ca^{2+}.[26] However, the mechanism by which binding of H^+ to its sensors in the RCK1 domain facilitates opening of the gate is not clear. The study here addresses the mechanism of activation of the Slo1 channel by H^+ in comparison with that by Ca^{2+} and illustrates the differential consequences of channel activation promoted by Ca^{2+} and H^+ mediated by the RCK1 domain.

Results

GV shift by intracellular H^+

Gating of the Slo1 channel is described by a multi-tier allosteric mechanism in which the VSDs and the intracellular ligand sensors regulate the conformation of the ion permeation gate in a

highly inter-dependent manner.[1, 5] Studies of Slo1 channel gating are often facilitated by examining channel function under those conditions in which contributions from one or more of the allosteric regulators are absent.[5] Following this approach, we compared the effects of H^+ and Ca^{2+} on gating properties of the human Slo1 channel expressed in HEK cells.

Our previous study showed that the pH_i dependence of macroscopic Slo1 current activation covers the pH_i range from ~7.5 to 6.0; the effect of H^+ on the voltage dependence is absent for $pH_i \geq 7.5$ and saturated at $pH_i = 5.7$ or lower.[25] The use of $pH_i < 6$ severely compromised the stability of the inside-out recording configuration at extreme voltages, and the results presented here utilized $pH_i = 6.2$. The current enhancing effect of H^+ at $pH_i = 6.2$ (Fig. 1A, B) is associated with a shift in $V_{0.5}$ of the GV curve to the negative direction (Fig. 1C) by 58.5 ± 3.2 mV (8) without markedly affecting Q_{app} (increased by 9.9 ± 4.0% (8)). The effect of H^+ on the GV was absent when His365 and His394 in the RCK1 domain were concurrently mutated to Arg or Ala (Fig. 1D), indicating that the $V_{0.5}$ shift is mediated by the aforementioned His residues in the RCK1 sensor. The results are consistent with the idea that the RCK sensor encompassing His365 and His394 bound with H^+ without divalent cations produces a shift in $V_{0.5}$ of ~−60 mV. The difference in $V_{0.5}$ between the Arg and Ala double mutants illustrate the importance of the electrostatic interaction involving the residues at positions 365 and 394.[26]

H^+ action on the Ca^{2+} bowl-defective Slo1 channel

Like H^+, Ca^{2+} also shifts $V_{0.5}$ to the negative direction and the high-affinity Ca^{2+} sensitivity of the Slo1 channel saturates at ≥ 100 μM.[27] Increasing $[Ca^{2+}]_i$ to 200 μM, a saturating concentration, produced a shift in $V_{0.5}$ of −202.5 ± 7.9 mV (5), more than 3 times greater than produced by H^+ at $pH_i = 6.2$ (Fig. 2A, B *left*). Molecularly, the −200 mV shift in $V_{0.5}$ by 200 μM Ca^{2+} includes contributions from the channel's RCK1 sensor and also the Ca^{2+} bowl sensor.[18, 27] Consistent with earlier results [18, 19], contemporaneous mutations in the two sensors (D362A:D367A:E399A:Δ894-895) essentially abolished the effect of Ca^{2+} up to 600 μM (data not shown; but see Piskorowski & Aldrich 28). Of the two sensors, the RCK1 sensor responds to H^+ and Ca^{2+} but the Ca^{2+} bowl sensor is not required for the H^+ sensitivity of the channel (Fig. 1D).[26] To examine the contribution from the RCK1 sensor in isolation, the pH_i dependence of the Ca^{2+} bowl-defective mutant (Slo1 Δ854-856) having the RCK1 sensor as the sole high-affinity Ca^{2+} sensor was examined. Consistent with the idea that this mutant channel has the Ca^{2+} bowl sensor disrupted, Ca^{2+} at 200 μM produced a shift in $V_{0.5}$ of −121.0 ± 4.3 mV (9), only ~60% of that observed in the wild-type channel (Fig. 2B *right*). However, the pH_i sensitivity of the mutant channel was similar to that of the wild-type channel; lowering pH_i from 7.5 to 6.2 produced a shift in $V_{0.5}$ of −50.6 ± 2.3 mV (9) (Fig. 2A, B *right*). Comparison of the changes in $V_{0.5}$ induced by high concentrations of H^+ and Ca^{2+} in the Ca^{2+} bowl-defective Slo1 Δ854-856 channel suggests that the RCK1 sensor with Ca^{2+} bound is more effective in promoting opening of the channel gate than the sensor bound with H^+.

Comparative effects of Ca^{2+} and H^+ on single-channel P_o

The effectiveness of the Ca^{2+} sensors of the Slo1 channel in stabilizing the open conformation of the gate is described by the allosteric coupling factor *C* in the gating model of Horrigan and Aldrich (HA model).[5] In this model, the equilibrium between the closed and the open conformations of the channel's permeation gate is described by the equilibrium constant *L*, which can be experimentally estimated by open probability (P_o) measurements in the absence of any ligand at negative voltages where the VSDs are at rest (Fig. 3C *top left*).[5] Furthermore, the HA model postulates that binding of Ca^{2+} to each of the four subunits in the channel increases the equilibrium constant *L* by *C* fold so that at a saturating concentration of Ca^{2+}, the equilibrium between the closed and open conformations of the gate is given by C^4*L (Fig. 3C *bottom left*). Accordingly, the ratio of P_o with a saturating concentration of Ca^{2+} to that without Ca^{2+} at negative voltages should correspond to C^4. The value of *C* has been estimated to be

~8 for the wild-type Slo1 channel with both the RCK1 and Ca^{2+} bowl sensors.[5] In the Ca^{2+} bowl-defective Slo1 Δ854-856 channel, increasing $[Ca^{2+}]_i$ to 200 μM at pH_i = 7.5 caused a ~50-fold increase in P_o at −160 mV (48.7 ± 16.6 (3)) and −120 mV (51.3 ± 8.3 (9)) (Fig. 3A, B), giving an estimate of 2.63 ± 0.092 (9) for *C* based on the results at −120 mV (Fig. 3C). In contrast, H^+ at pH_i = 6.2 effected only a 3-fold increase in P_o at −120 mV (3.14 ± 089 (11)). These results demonstrate that like Ca^{2+}, H^+ acts to stabilize the channel's permeation gate, but suggest H^+ may be less efficacious than Ca^{2+}, in line with the finding that the shift in $V_{0.5}$ is greater for Ca^{2+} than pH (Fig. 2).

It is clear from Figs. 3A and 3B that H^+ at pH 6.2 is less effective than 200 μM Ca^{2+} in stabilizing the open conformation; however, these results may underestimate the effect of protons on the RCK1 sensor for the following two reasons. First, it was necessary to use a sub-saturating concentration of H^+ (pH_i = 6.2) to maintain patch stability. Therefore, the data in Fig. 3B place only a lower limit on the value of C of 1.26 ± 0.072 (11) (Fig. 3C) because the observed increase in P_o at −120 mV should be less than *C*[4]. Additional evidence suggests that the activating effect of H^+ at RCK1 may be partially masked by an inhibitory effect at an unidentified site. In the presence of the double mutation H365R:H394R or H365A:H394A, which removes the sensitivity of macroscopic $V_{0.5}$ to pH_i, lowering pH_i from 7.5 to 6.2 did not increase P_o at negative voltages (Fig. 3D), affirming that the P_o increase observed in the Ca^{2+} bowl-defective mutant (Fig. 3B) is mediated by the RCK1 sensor. In fact, H^+ at pH_i = 6.2 actually decreased P_o at negative voltages for the double mutants H365R:H394R and H365A:H394A to 44.7 ± 6.3% (7) and 43.4 ± 11.1% of the control values ($P < 0.035$; Fig. 3D), respectively. The decrease in P_o in the His double mutants to ~44% of the control level suggests that the stimulatory effect of H^+ on P_o mediated specifically by His365 and His394 may be in fact greater than that estimated from the Ca^{2+} bowl-defective mutant and accordingly the value of *C* mediate by His365 and His394 may be greater than ~1.63.

Differences in the coupling factor C may be sufficient to explain macroscopic GV shifts by Ca^{2+} and H^+

Because H^+ and Ca^{2+} appear to act by similar mechanisms, we evaluated whether the differences in the value of the HA model parameter *C*, which describes the strength of coupling between the ligand sensor and the channel's gate (Fig. 3C), are sufficient to account for the shifts in macroscopic $V_{0.5}$ caused by Ca^{2+} and H^+. In the case of Ca^{2+}, simulations using the value of $C = 2.6$ estimated from the effect of Ca^{2+} on the single-channel P_o for the Ca^{2+} bowl-defective mutant produced a shift in $V_{0.5}$ by 200 μM Ca^{2+} of ~−95 mV (Fig. 4A), which is similar, albeit not identical, to the measured shift in $V_{0.5}$ of −120 mV (see Fig. 2B). In the case of H^+, we fit G-V relations at different pH_i from pH 7.5 to 6.2 with the HA model (Fig. 4B) yielding parameter values for H^+-dependent activation of $C = 2.14 \pm 0.08$ and $K_D = 1.31 \pm 0.18\ \mu M$. The predicted relationship between $V_{0.5}$ and pH_i (Fig. 4C) suggests that protonation of the RCK1 site may not saturate until pH ~5, and the estimated value of $C = 2.14$ is therefore considerably larger than the lower-limit ($C > 1.26$) estimated from the 3.14-fold increase in P_o at −120 mV at pH 6.2. Importantly, however, the model parameters for H^+ are consistent with the data at pH 6.2 since they not only reproduce the approximate −50 mV G-V shift from pH 7.5 to 6.2 but also a 3.97-fold increase in P_o at −120 mV. Thus, we conclude that differences in the values of *C* for H^+ and Ca^{2+} together with sub-saturating levels of protons at pH 6.2 are sufficient to account for the different effects of these ligands on steady-state activation.

The HA model contains an additional coupling factor *E*, representing a weak allosteric interaction between ligand-binding and voltage-sensor activation. For simplicity, the value of *E* in all simulations was fixed to the value (2.4) determined previously for Ca^{2+}.[5] However, there was also some evidence that the *E* factor is required to account for the effect of H^+. While the pH dependence of $V_{0.5}$ could be fit by eliminating this interaction ($E = 1$) and increasing

C to 3.23 (data not shown), these parameters greatly overestimate the change in P_o at −120 mV at pH 6.2, by 2.7-fold. Thus, H^+ may also act like Ca^{2+} to increase voltage-sensor activation.

Ca^{2+} and H^+ have a greater impact on the opening rate constant

The increase in P_o by Ca^{2+} or H^+, as the result of an increase in the coupling factor *C*, could involve an increase in the overall opening rate and/or a decrease in the closing rate. At the negative voltages utilized in our experiments, gating of the Slo1 channel is well described by a simple two-state model, a subset of the HA model, with the effective opening rate constant δ_0 and the closing rate constant γ_0 (Fig. 5C *left*). Consistent with the two-state kinetics, the measured open durations were indeed adequately described by a single exponential (Fig. 5A). The two-state kinetics allowed us to estimate the values of the two rate constants using the changes in P_o and the mean open time. Both Ca^{2+} at 200 μM and H^+ at $pH_i = 6.2$ increased the mean open duration ($P < 0.035$; Fig. 5A) but the fractional increase by 200 μM Ca^{2+} was significantly greater ($P < 0.0008$). The changes in mean open duration (Fig. 5B) corresponded to 33% and 11% decrease in the value of the closing rate constant γ_0 by Ca^{2+} and H^+ (Fig. 5C). Additionally, using the γ_0 and P_o values, we estimated that Ca^{2+} increased the value of the opening rate constant δ_0 by 34.4 ± 6.0 (9) fold whereas H^+ increased the rate constant value by only 2.7 ± 0.7 (10) fold, less than 10% of the increase by Ca^{2+} (Fig. 5C). Both Ca^{2+} and H^+ have a greater influence on the opening rate constant δ_0 than on the closing rate constant γ_0 and the changes by Ca^{2+} are greater than those by H^+.

Macroscopic activation and deactivation kinetics

The results of the single-channel analysis that Ca^{2+} is more effective than H^+ in decreasing the closing rate constant γ_0 and also in increasing the opening rate constant δ_0 suggest that the two RCK1 sensor ligands may differentially regulate the channel's macroscopic kinetics. Specifically, 200 μM Ca^{2+} should slow the macroscopic deactivation kinetics and accelerate the activation kinetics more effectively than pH 6.2 if the single-channel results obtained at negative voltages can be extrapolated to positive voltages. We therefore compared the changes in macroscopic kinetics caused by $pH_i = 6.2$ and 200 μM Ca^{2+} in the Ca^{2+} bowl-defective Slo1 Δ854-856 channel (Fig. 6). Both Ca^{2+} at 200 μM and H^+ at $pH_i = 6.2$ slowed the deactivation kinetics (Fig. 6A *left*) and accelerated the activation kinetics (Fig. 6A *right*). Comparison of the fractional changes in the activation and deactivation time constant values (Fig. 6B) showed that Ca^{2+} at 200 μM was more effective than H^+ in regulating the channel kinetics. At negative voltages (≤−120 mV), Ca^{2+} increased the deactivation time constant by ~100% in a relatively voltage-independent manner whereas H^+ at $pH_i = 6.2$ increased the time constant by only ~50% (Fig. 6C). Similarly, at positive voltages (≥120 mV), Ca^{2+} had a noticeably greater effect than H^+ in decreasing the mean activation time constant; Ca^{2+} decreased the time constant down to ~10% and H^+ decreased it to ~30% of the value without Ca^{2+} at $pH_i = 7.5$ in a voltage-independent manner (≥120 mV). The steepness of the voltage dependence of the time constant at negative (≤−120 mV) and positive (≥180 mV) was not markedly altered by Ca^{2+} at 200 μM or H^+ at $pH_i = 6.2$ compared with that at $pH_i = 7.5$ without Ca^{2+}. However, a simple shift of the voltage dependence of the time constant observed at $pH_i = 7.5$ without Ca^{2+} to the negative direction by −50.6 mV (Fig. 6B dashed curve), the $V_{0.5}$ change caused by H^+ at $pH_i = 6.2$ (Fig. 2), did not match the voltage dependence of the time constant at $pH_i = 6.2$ especially at positive voltages (>150 mV); the acceleration of the activation kinetics by H^+ at $pH_i = 6.2$ was more pronounced than that predicted by the simple shift along the voltage axis, as is the case for Ca^{2+} (Fig. 6B)[5], H^+ at $pH_i = 6.2$ did not alter macroscopic current kinetics in the H365R:H394R and H365A:H394A channels in the voltage range of −220 to 270 mV (Fig. 6D), confirming that the changes in the macroscopic current kinetics are mediated by His365 and His394 in the RCK1 sensor.

Titration of the voltage dependence of activation by Ca^{2+} and H^+

To better characterize how H^+ and Ca^{2+} regulate the channel kinetics, we titrated the macroscopic $V_{0.5}$ of the Ca^{2+} bowl-defective Slo1 channel by manipulating pH_i and $[Ca^{2+}]_i$ so that the current kinetics could be compared when their $V_{0.5}$ values are equal. We found that the $V_{0.5}$ and Q_{app} values with 10 μM Ca^{2+} at pH_i =7.5 were indistinguishable from those at pH_i = 6.2 without Ca^{2+} ($P \geq 0.44$; Fig. 7A). While H^+ at pH_i = 6.2 and Ca^{2+} at 10 μM produced statistically indistinguishable shifts in $V_{0.5}$, the effects on the kinetics of the channel were clearly different. H^+ at pH_i = 6.2 accelerated the activation kinetics to a greater extent than Ca^{2+} at 10 μM (Fig. 7B, C, D). For example, at 270 mV (Fig. 7B *right*), H^+ at pH_i = 6.2 decreased the time constant of activation to ~30% of the control value (Fig. 7C, D red) while Ca^{2+} at 10 μM at pH_i = 7.5 decreased the activation time constant to ~60% (Fig. 7C, D; black). At ≥200 mV, both H^+ and Ca^{2+} decreased the activation time constant without markedly altering its voltage dependence. Both H^+ and Ca^{2+} slowed the deactivation kinetics at ≤ 0 mV in the Ca^{2+} bowl-defective mutant. However, in contrast with the results at positive voltages, H^+ and Ca^{2+} were equally potent in slowing the deactivation kinetics (Fig. 7B–D). These observations about the changes in kinetics in the Ca^{2+} bowl-defective Slo1 channel with Ca^{2+} at 10 μM are consistent with the results of Zeng et al.[19] Similar titration procedures using the wild-type channel with both the RCK1 and Ca^{2+} bowl sensors (Fig. 7E–H) showed that H^+ at pH_i = 6.2 and Ca^{2+} at 1 μM produced indistinguishable shifts in $V_{0.5}$ and that the comparative effects of H^+ and Ca^{2+} on the wild-channel were similar to those observed in the Ca^{2+} bowl mutant channel with 10 μM Ca^{2+}.

Titration of the voltage dependence of activation by Mg^{2+} and H^+

As performed using Ca^{2+}, we titrated the macroscopic $V_{0.5}$ of the wild-type channel using Mg^{2+}, another intracellular ligand of the Slo1 channel. [17, 18] The Mg^{2+}-sensitivity is mediated by a mechanism distinct from that underlying the activation by Ca^{2+}. [17, 18, 29, 30] We found that Mg^{2+} at 6 mM induces the same shift in $V_{0.5}$ as that by lowering pH_i to 6.2 without Ca^{2+} (Supplementary Figure 1A). However, H^+ at pH_i = 6.2 more effectively accelerated that activation kinetics than Mg^{2+} at 6 mM (Supplementary Figure 1B, C).

Discussion

Open probability and the kinetics of the Slo1 BK channel are finely regulated by binding of ion ligands such as Ca^{2+}, Mg^{2+} and H^+, to their respective sensors in the cytoplasmic RCK1 and RCK2 domains.[1, 19, 22] We showed previously that H^+, acting via the high-affinity RCK1 Ca^{2+} sensor, dramatically increases Slo1 macroscopic currents.[22, 25] In this study, we examined the mechanism of the channel activation by H^+ mediated through the RCK1 sensor in comparison with that by Ca^{2+}.

Steady-state activation properties

Gating of the Slo1 channel is well described by a multi-tier allosteric mechanism in which activation of voltage and ligand sensors stabilizes the open conformation of the channel's ion permeation gate. The gate can also influence the sensors in a reciprocal manner. For example, according to the HA model[5], the equilibrium constant L describes the closed-open equilibrium of the channel's gate in the absence of allosteric influences from the voltage and ligand sensors, and the open state occupancy becomes more probable by C^4 folds when all Ca^{2+} sensors in the four subunits are saturated with Ca^{2+}. Mutagenesis studies suggest that each Slo1 subunit most probably harbors two high-affinity Ca^{2+} sensors, the RCK1 sensor and the Ca^{2+} bowl sensor. [15, 18–20] Using the Ca^{2+} bowl-defective Slo1 mutant with the RCK1 sensor intact, our measurements of the single-channel activity at negative voltages where VSD activation should be negligible show that the value of C for Ca^{2+} acting through the RCK1 sensor is ~2.6, representing about 50% of the energetic effect of Ca^{2+} on the wild-type channel.[5] Thus, when

one RCK sensor contains Ca^{2+}, the open state occupancy is stabilized by 0.57 kcal/mole ($\Delta G = kT \ln(C)$) and H^+ at pH 6.2 is about 25 to 50% as effective in stabilizing the open state based on the effect on P_o at-120 mV (C = 1.26–1.63). However, full occupancy by H^+ may be almost 80% as effective as Ca^{2+} or ΔG = 0.46 kcal/mol, based on a value of C = 2.14 estimated from the pH dependence of $V_{0.5}$ (Fig. 4B).

Simulations based on the HA model suggest differences in the value of C for Ca^{2+} (2.6) and H^+ (2.14) are sufficient to account for both the observed shifts in macroscopic GV curves as well as change in single-channel P_o at negative voltages by 200 μM Ca^{2+} or pH_i 6.2. Therefore, the different actions of these ligands can be primarily attributed to their ability to stabilize the open conformation. However, we cannot rule out minor contributions from two additional mechanisms. First, an unanticipated inhibitory effect of H^+ may mask the stimulatory effect of H^+. In the absence of His365 and His394, H^+ at pH_i = 6.2 decreases P_o by ~56%. The molecular mechanism and locus responsible for this inhibitory effect are not clear but the overall consequence is underestimation of the value of C. Second, our study did not address whether H^+ changes the strength of allosteric coupling between the RCK1 sensor and the VSDs. Multiple lines of evidence, including gating current measurements, suggest that VSD activation is facilitated when Ca^{2+} is bound to the ligand sensors.[5] The strength of the coupling conferred by Ca^{2+} is described by the parameter E in the HA model and estimated to be 2.4 for the wild-type channel. It is conceivable that H^+ also alters the value of the parameter E. However, the data suggest a value of E similar to that for Ca^{2+} is necessary to account for both the changes in $V_{0.5}$ and P_O at −120 mV at pH 6.2.

Structural rearrangements within the RCK1 sensor

Protonation of His365 and His394 has been proposed to drive Slo1 channel activation through electrostatic interaction with nearby charged residues including Asp367 in the RCK1 site because the effect of pH_i is reduced by mutation of Asp367 or increased ionic strength.[26] Given that H^+ alters the C-O equilibrium, this electrostatic mechanism suggests that the distance between the two His residues and Asp367 may decrease during opening of the ion permeation gate. To determine if such a mechanism is compatible with our results, we first calculated how large a movement would be required to account for the full energetic effect of H^+ on channel opening, ΔG = 0.46 kcal/mol. The change in free energy involved in moving 2 positive charges (His365 and His394) from a distance R_C to R_O relative to Asp367 is:

$$\Delta G = 2 e_0 [V(R_c) - V(R_o)]$$

where V(r), the electrostatic potential of Asp367, can be approximated by the Debye-Hückel expression:

$$V(r) = q_1 \frac{\exp(-\kappa r)}{4\pi\varepsilon_0\varepsilon_r r} \text{ and } \kappa^{-1} \text{ is the Debye length: } \kappa^{-1} = \sqrt{\frac{\varepsilon_0\varepsilon_r RT}{2F^2 I}}$$

where $\varepsilon_0 = 8.85\times10^{-12}$ C^2/Jm, ε_r = 80, R = 8.31 J/mol.K, T = 293 K, F = 9.65×10^4 C/mol, and I = ionic strength. If we assume an initial distance R_C = 7 Å in the closed state (the approximate Debye length in our standard recording solutions with I = 0.18 M), then a distance change of only 2.2 Å (R_O = 4.8 Å) would be sufficient to account for C = 2.1. This estimate assumes an aqueous dielectric constant, consistent with the interaction of surface-exposed charged groups on proteins.[31]

A similar result was obtained when we fit the dependence of $\Delta V_{0.5}$ in response a change in pH_i to 6.2 on ionic strength using the Debye-Hückel expression (Fig. 8). In this case, the

relationship between the magnitude of $\Delta V_{0.5}$ and ΔG cannot be determined exactly because $\Delta V_{0.5}$ reflects energetic effects of H^+ on both the C-O transition (allosteric coupling factor *C*) and VSD activation (coupling factor *E*). Therefore, we fit the data with the HA model using two different assumptions about the effect on ionic strength on *C* and *E*. In the first case (Fig. 8, solid curve), we assumed that the *E* factor is constant whereas the *C* factor (ΔG) varies with ionic strength according to the Debye-Hückel expression, yielding values of $R_C = 8.8 \pm 0.7$ Å and $R_O = 5.4 \pm 0.5$ Å. In the second case (Fig. 8, dotted curve), we assumed that *C* and *E* are both sensitive to ionic strength, reflecting electrostatic interaction of His365 and His394 with two equidistant point charges in the RCK1 site and VSD respectively, yielding values of $R_C = 5.7 \pm 0.3$ Å and $R_O = 4.2 \pm 0.2$ Å. Although there is some ambiguity in these fits because of assumptions about interaction with the VSD, the apparent insensitivity of $\Delta V_{0.5}$ to $I \leq 0.18$ M requires that the distances involved are similar to the 7 Å Debye length at I = 0.18 M. Therefore, consistent with the earlier suggestion[26], it is reasonable that His365 and His394 are in close proximity to other charged groups in or near the RCK1 site. Thus, two different methods suggest that subtle movements of these groups relative to each other during channel opening would be sufficient to account for the observed energetic effect of H^+ on channel opening. A critical test of this idea awaits availability of experimentally-derived structural information on the RCK1 sensor.

Comparative effects of Ca^{2+} and H^+

The notion that subtle conformational changes occur within the RCK1 sensor during channel opening promoted by H^+ is implicit in allosteric models like the HA model, which assumes that the ligands can bind to both open and closed channels but do so with higher affinity to the open conformation. In the HA model, opening of the channel's gate increases the effective affinity of each sensor by *C* folds. Therefore, the smaller value of *C* estimated for H^+ than that for Ca^{2+} implies a smaller difference in ligand binding affinity between the closed and open conformations of the channel with H^+ than Ca^{2+}. This energetic difference may be related to how the two ligands are coordinated by the RCK1 sensor. Binding of Ca^{2+} to the RCK1 sensor most probably requires multiple structural elements such that any change in the binding site during opening could geometrically perturb the coordination. In contrast, changes in H^+ affinity imply a change in pK_a of the binding sites (His365 and His394), which is expected to be more readily influenced by electrostatic interactions than geometric considerations. The contrasting requirements for binding of Ca^{2+} and H^+ may contribute to the differential sensitivity of the RCK1 sensor to the channel's gate status and underlie the markedly different efficacies of the two ligands as measured by $V_{0.5}$ changes.

A decrease in pH_i by one unit, which may occur following brain ischemia[32], is as effective as 1 μM Ca^{2+} in the wild-type channel and 10 μM Ca^{2+} in the Ca^{2+} bowl deletion mutant channel in shifting $V_{0.5}$ to the negative direction. At these concentrations, despite their equipotency in shifting $V_{0.5}$, H^+ and Ca^{2+} have very distinct effects on the channel kinetics. H^+ is noticeably more effective than Ca^{2+} in accelerating the activation kinetics in response to depolarization; comparison of the activation time constant shows that the channel gate opens nearly twice as fast with H^+. The kinetics of the channel opening promoted by H^+ is also faster than that by Mg^{2+}. It is not, however, possible to pinpoint the biophysical basis of the greater acceleration by H^+ because multiple allosteric interactions are at play. For example, the effect could be mediated directly through the RCK1 sensor's coupling to the gate or indirectly via the channel's VSDs. Regardless of the underlying mechanism, the RCK1 sensor has a capability to encode the nature of the bound ligand and transmits qualitatively different information to the channel's gate.

Possible physiological and pathophysiological implications

The multiplex nature of the coupling between the RCK1 sensor and the channel gate, controlling the kinetics and steady-state activation properties differentially, most probably contributes to the well-known functional diversity of the Slo1 BK channel.[8] Such an arrangement allows the Slo1 BK channel to participate in numerous physiological and pathophysiological phenomena occurring over different time scales and in different tissues, from determination of action potential duration[33] to regulation of vascular smooth muscle tone.[34] For example, in hippocampal neurons, transient activation of Slo1 BK channel complexes plays a role in frequency-dependent broadening of action potentials such that BK channel inhibitors increase the spike duration and abate further frequency-dependent broadening.[35] The spike broadening is enhanced by high intracellular concentrations of exogenous pH buffers[36], suggesting that the H^+-mediated activation of the RCK1 sensor normally acts to minimize spike broadening. The multi-ligand characteristic of the RCK1 sensor may also come into play during ischemia, which is accompanied by changes in intracellular concentrations of many ions with distinct time courses.[23, 24] Typically, intracellular acidosis, up to one pH unit[32], an increase in $[Na^+]$ and a decrease in [ATP], are first observed, followed by a delayed increase in $[Ca^{2+}]_i$.[23, 24] Intracellular $[Mg^{2+}]$ also increases.[24] The rapid acidosis during ischemia suggests that activation of Slo1 BK channel complexes by H^+ mediated by the RCK1 sensor may represent a first line of defense during an early phase of ischemic injury. With prolonged ischemia, $[Ca^{2+}]$ increases and Ca^{2+}-dependent activation of the channel may become dominant, leading to greater activation of the channels. It is interesting to note that the increases in $[H^+]$, $[Ca^{2+}]$ and $[Mg^{2+}]$ known to be associated with ischemia[24] all promote opening of the Slo1 BK channel, further reinforcing the notion that the Slo1 BK channel plays a protective role during ischemic insults. Differential consequences of activation of Slo1 BK channels by these intracellular ligands may allow the channels to respond appropriately to different phases of ischemia. The kinetics of the Slo1 BK channel complex plays important functional roles in the nervous system where fast signaling is often required. The importance of the channel kinetics is well illustrated in a study examining the mechanism of the epilepsy-causing mutation D369G (using the numbering in AAB65837 used in this study) in the RCK1 sensor.[11] Thus, the pH_i sensitivity of the Slo1 channel may be particularly important in the neuronal function.

Methods

Channel expression

Wild-type and mutant human Slo1 channels (U11058/AAB65837) were transiently expressed in HEK tsA cells using plasmid DNAs. Electrophysiological measurements were performed 24 to 48 hrs later as described previously.[22]

Electrophysiology

Macroscopic and single-channel currents were measured in the inside-out configuration using an Axopatch 200B (Molecular Devices, Sunnyvale, CA) amplifier as described.[37] For macroscopic current measurements, recording electrodes had a typical initial resistance of 1 MΩ when used with the solutions described below, and 50 to 60% of the initial input resistance was electronically compensated. Macroscopic leak and capacitative currents were subtracted with a P/6 protocol using the leaking holding voltage of −50 mV. Both macroscopic and single-channel currents were filtered at 10 kHz through the built-in filter of the amplifier and digitized at 100 kHz. Voltage pulses were applied every 3 s or greater.

Data analysis

Macroscopic currents were analyzed using custom routines implemented in IgorPro (Wavemetrics, Lake Oswego, OR) running on Mac OS as described.[37, 38] Typically, voltage dependence of macroscopic conductance (GV) was estimated from the extrapolated sizes of the instantaneous tail currents at −40 mV following pulses to different voltages and fitted with a Boltzmann function as a data descriptor function. Each GV was characterized by its half-activation voltage ($V_{0.5}$) and apparent charge movement (Q_{app}). Activation and deactivation kinetics were characterized by fitting the currents with a single exponential excluding the initial 250 μs and 160 μs, respectively. The voltage dependence of the time constant was in turn fitted with the equation $\tau(V)= \tau_0*\exp(qV/k_BT)$ where $\tau(V)$ is the time constant at voltage V, τ_0 is the time constant value at 0 mV, q is the partial charge value, and k_B and T have their usual meanings. Single-channel open probability was estimated using all-point amplitude histograms and corrected for the number of channels present in each patch. The number of channels present was determined using the macroscopic peak current size at ≥220 mV and the single-channel current-voltage relation estimated using voltage ramps as described.[37] Single-channel open probability values obtained at low pH_i, with Ca^{2+} and Mg^{2+}, were normalized to the control values obtained at $pH_i = 7.5$ without any Ca^{2+} and referred to as P_o ratios. This normalization was necessary as the variability in the estimated absolute open probability values at negative voltages was high, often ranging from 1×10^{-7} to 2×10^{-6} at −120 mV on a given day of experiments. Single-channel dwell times were measured as described previously[39] and were not corrected for the left-censor time of the recording system.

The parameter *C* in the allosteric gating model of Horrigan and Aldrich (HA model)[5] was estimated from single-channel open probability measurements at negative voltages where VSD activation is negligible, typically −160 or −120 mV. These voltages were deemed sufficiently negative as the mean $V_{0.5}$ value with 200 μM Ca^{2+} is ≥ 50 mV even in the Ca^{2+} bowl-defective channel studied (Δ854-855). At these voltages, intracellular Mg^{2+}, whose stimulatory effect requires VSD activation[30], does not increase open probability (Supplementary Figure 2). The values of the remaining HA model parameters were taken from Horrigan et al[37] developed for the wild-type Slo1 channel. The simulated GV curves were shifted by along the voltage axis by 35 mV to match the $V_{0.5}$ value of the Ca^{2+} bowl-mutant channel. Because detailed information about the K_D value for H^+ of the RCK1 sensor is unavailable, the ligand sensor K_D value for H^+ in the HA model was set to 0.35 μM[25]. Simulations using the HA model were performed with IgorPro.

The results are presented as mean ± SEM (n), where n is the number of independent measurements. Means of two groups were compared using Student's t-test or paired Student's t-test. When appropriate, the results of multi-mean comparisons were corrected using the Bonferroni method. The differences were considered significant when *P* values were < 0.05. Statistical tests were performed using IgorPro or DataDesk (DataDescription, Ithaca, NY). The equation fit parameter values are presented as mean ± 95% confidence interval as implemented in IgorPro.

Solutions

The external solution contained (in mM): 140 KCl, 2 $MgCl_2$, 10 HEPES, pH 7.2 with *N*-methyl-*D*-glucamine (NMDG). The internal solution with $pH_i = 7.5$ and 0 μM Ca^{2+} contained (in mM): 140 KCl, 11 EDTA, 0.02 crown-ether(+)-18-crown-6-tetra-carboxylic acid (18C6TCA)[40], 10 HEPES, pH = 7.5 with NMDG. The internal solution with $pH_i = 6.2$ and 0 μM Ca^{2+} was made by substituting 10 mM HEPES with 10 mM MES. The internal solution with $pH_i = 7.5$ and 1 μM Ca^{2+} contained (in mM): 140 KCl, 3.7 HEDTA, 3.7 $CaCl_2$, 10 HEPES, pH 7.5 with NMDG. The internal solution with $pH_i = 7.7$ and 10 μM Ca^{2+} was made with 9 mM $CaCl_2$. The internal solution with $pH_i = 7.5$ and 6 mM Mg^{2+} contained (in mM): 140 KCl, 11 EGTA, 6 $MgCl_2$,

0.02 18C6TCA, 10 HEPES, pH = 7.5 with NMDG. The solution with 200 μM Ca^{2+} did not contain any EGTA or EDTA.

Supplementary Material

Refer to Web version on PubMed Central for supplementary material.

Acknowledgments

The study was supported in part by NIH, TMWFK (PE114-1) and DFG (HE 2993/8).

Abbreviations

VSD	voltage-sensor domain
RCK	regulator of conductance for K^+
GV	conductance-voltage
IV	current-voltage
P_o	open probability

References

1. Magleby KL. Gating mechanism of BK (Slo1) channels: so near, yet so far. J Gen Physiol 2003;121:81–96. [PubMed: 12566537]
2. Rothberg BS. Allosteric modulation of ion channels: the case of maxi-K. Sci STKE 2004 2004:pe16.
3. Jan LY, Jan YN. Ways and means for left shifts in the MaxiK channel. Proc Natl Acad Sci U S A 1997;94:13383–5. [PubMed: 9391031]
4. Horrigan FT, Aldrich RW. Allosteric voltage gating of potassium channels II. mslo channel gating charge movement in the absence of Ca^{2+} J Gen Physiol 1999;114:305–36. [PubMed: 10436004]
5. Horrigan FT, Aldrich RW. Coupling between voltage sensor activation, Ca^{2+} binding and channel opening in large conductance (BK) potassium channels. J Gen Physiol 2002;120:267–305. [PubMed: 12198087]
6. Rothberg BS, Magleby KL. Gating kinetics of single large-conductance Ca^{2+}-activated K^+ channels in high Ca^{2+} suggest a two-tiered allosteric gating mechanism. J Gen Physiol 1999;114:93–124. [PubMed: 10398695]
7. Kaczorowski GJ, Knaus HG, Leonard RJ, McManus OB, Garcia ML. High-conductance calcium-activated potassium channels; structure, pharmacology, and function. J Bioenerg Biomembr 1996;28:255–67. [PubMed: 8807400]
8. Salkoff L, Butler A, Ferreira G, Santi C, Wei A. High-conductance potassium channels of the SLO family. Nat Rev Neurosci 2006;7:921–31. [PubMed: 17115074]
9. Du W, Bautista JF, Yang H, Diez-Sampedro A, You SA, Wang L, et al. Calcium-sensitive potassium channelopathy in human epilepsy and paroxysmal movement disorder. Nat Genet 2005;37:733–8. [PubMed: 15937479]
10. Seibold MA, Wang B, Eng C, Kumar G, Beckman KB, Sen S, et al. An African-specific functional polymorphism in KCNMB1 shows sex-specific association with asthma severity. Hum Mol Genet. 2008
11. Wang B, Rothberg BS, Brenner R. Mechanism of increased BK channel activation from a channel mutation that causes epilepsy. J Gen Physiol 2009;133:283–94. [PubMed: 19204188]
12. Shen KZ, Lagrutta A, Davies NW, Standen NB, Adelman JP, North RA. Tetraethylammonium block of Slowpoke calcium-activated potassium channels expressed in *Xenopus* oocytes: evidence for tetrameric channel formation. Pflügers Archiv 1994;426:440–5.
13. Ma Z, Lou XJ, Horrigan FT. Role of charged residues in the S1-S4 voltage sensor of BK channels. J Gen Physiol 2006;127:309–28. [PubMed: 16505150]

14. Jiang Y, Pico A, Cadene M, Chait BT, MacKinnon R. Structure of the RCK domain from the *E. coli* K^+ channel and demonstration of its presence in the human BK channel. Neuron 2001;29:593–601. [PubMed: 11301020]
15. Yusifov T, Savalli N, Gandhi CS, Ottolia M, Olcese R. The RCK2 domain of the human BK_{Ca} channel is a calcium sensor. Proc Natl Acad Sci U S A 2008;105:376–81. [PubMed: 18162557]
16. Jiang Y, Lee A, Chen J, Cadene M, Chait BT, MacKinnon R. Crystal structure and mechanism of a calcium-gated potassium channel. Nature 2002;417:515–22. [PubMed: 12037559]
17. Shi J, Krishnamoorthy G, Yang Y, Hu L, Chaturvedi N, Harilal D, et al. Mechanism of magnesium activation of calcium-activated potassium channels. Nature 2002;418:876–80. [PubMed: 12192410]
18. Xia XM, Zeng X, Lingle CJ. Multiple regulatory sites in large-conductance calcium-activated potassium channels. Nature 2002;418:880–4. [PubMed: 12192411]
19. Zeng XH, Xia XM, Lingle CJ. Divalent cation sensitivity of BK channel activation supports the existence of three distinct binding sites. J Gen Physiol 2005;125:273–86. [PubMed: 15738049]
20. Schreiber M, Salkoff L. A novel calcium-sensing domain in the BK channel. Biophys J 1997;73:1355–63. [PubMed: 9284303]
21. Sweet TB, Cox DH. Measurements of the BK_{Ca} channel's high-affinity Ca^{2+} binding constants: effects of membrane voltage. J Gen Physiol 2008;132:491–505. [PubMed: 18955592]
22. Hou S, Xu R, Heinemann SH, Hoshi T. Reciprocal regulation of the Ca^{2+} and H^+ sensitivity in the SLO1 BK channel conferred by the RCK1 domain. Nat Struct Mol Biol 2008;15:403–10. [PubMed: 18345016]
23. Silver IA, Erecinska M. Intracellular and extracellular changes of $[Ca^{2+}]$ in hypoxia and ischemia in rat brain in vivo. J Gen Physiol 1990;95:837–66. [PubMed: 2163431]
24. Murphy E, Steenbergen C. Ion transport and energetics during cell death and protection. Physiology (Bethesda) 2008;23:115–23. [PubMed: 18400694]
25. Avdonin V, Tang XD, Hoshi T. Stimulatory action of internal protons on Slo1 BK channels. Biophys J 2003;84:2969–80. [PubMed: 12719228]
26. Hou S, Xu R, Heinemann SH, Hoshi T. The RCK1 high-affinity Ca^{2+} sensor confers carbon monoxide sensitivity to Slo1 BK channels. Proc Natl Acad Sci U S A 2008;105:4039–43. [PubMed: 18316727]
27. Qian X, Niu X, Magleby KL. Intra- and intersubunit cooperativity in activation of BK channels by Ca^{2+} J Gen Physiol 2006;128:389–404. [PubMed: 17001085]
28. Piskorowski R, Aldrich RW. Calcium activation of BK_{Ca} potassium channels lacking the calcium bowl and RCK domains. Nature 2002;420:499–502. [PubMed: 12466841]
29. Yang H, Hu L, Shi J, Delaloye K, Horrigan FT, Cui J. Mg^{2+} mediates interaction between the voltage sensor and cytosolic domain to activate BK channels. Proc Natl Acad Sci U S A 2007;104:18270–5. [PubMed: 17984060]
30. Horrigan FT, Ma Z. Mg^{2+} enhances voltage sensor/gate coupling in BK channels. J Gen Physiol 2008;131:13–32. [PubMed: 18166624]
31. Lee KK, Fitch CA, Garcia-Moreno EB. Distance dependence and salt sensitivity of pairwise, coulombic interactions in a protein. Protein Sci 2002;11:1004–16. [PubMed: 11967358]
32. Lipton P. Ischemic cell death in brain neurons. Physiol Rev 1999;79:1431–568. [PubMed: 10508238]
33. Storm JF. Action potential repolarization and a fast after-hyperpolarization in rat hippocampal pyramidal cells. J Physiol (Lond) 1987;385:733–59. [PubMed: 2443676]
34. Nelson MT, Cheng H, Rubart M, Santana LF, Bonev AD, Knot HJ, et al. Relaxation of arterial smooth muscle by calcium sparks. Science 1995;270:633–7. [PubMed: 7570021]
35. Shao LR, Halvorsrud R, Borg-Graham L, Storm JF. The role of BK-type Ca^{2+}-dependent K^+ channels in spike broadening during repetitive firing in rat hippocampal pyramidal cells. J Physiol (Lond) 1999;521:135–46. [PubMed: 10562340]
36. Tombaugh GC. Intracellular pH buffering shapes activity-dependent Ca^{2+} dynamics in dendrites of CA1 interneurons. J Neurophysiol 1998;80:1702–12. [PubMed: 9772233]
37. Horrigan FT, Heinemann SH, Hoshi T. Heme regulates allosteric activation of the Slo1 BK channel. J Gen Physiol 2005;126:7–21. [PubMed: 15955873]

38. Tang XD, Daggett H, Hanner M, Garcia ML, McManus OB, Brot N, et al. Oxidative regulation of large conductance calcium-activated potassium channels. J Gen Physiol 2001;117:253–74. [PubMed: 11222629]

39. Avdonin V, Hoshi T. Modification of voltage-dependent gating of potassium channels by free form of tryptophan side chain. Biophys J 2001;81:97–106. [PubMed: 11423398]

40. Neyton J. A Ba^{2+} chelator suppresses long shut events in fully activated high-conductance Ca^{2+}-dependent K^{+} channels. Biophys J 1996;71:220–6. [PubMed: 8804605]

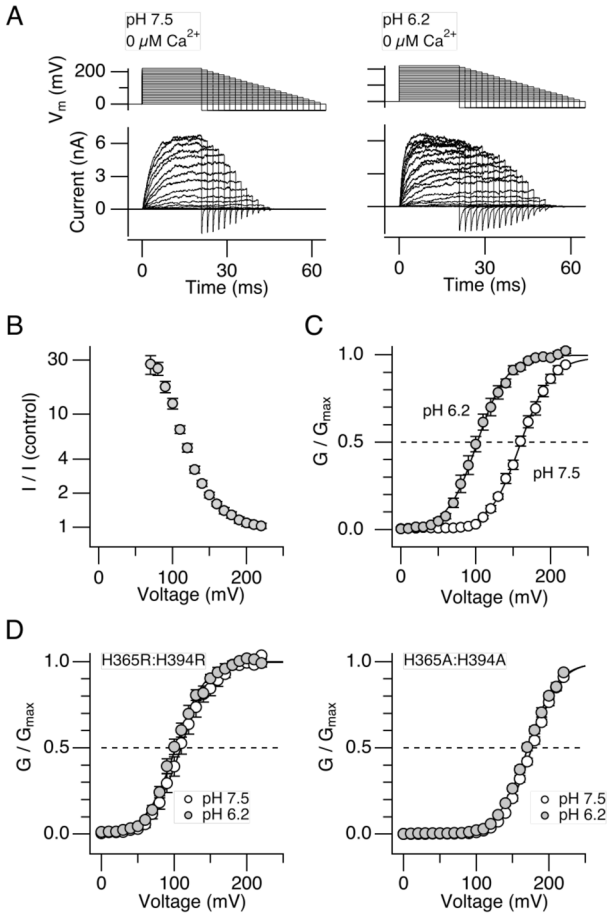

Figure 1.

H^+ enhances Slo1 currents in the absence of divalent cations in a His365- and His394-dependent manner. A. Representative macroscopic currents recorded at pH_i = 7.5 (*left*) and pH_i = 6.2 (*right*) without Ca^{2+}. B. Voltage dependence of the fractional increase in the peak outward current size by pH_i = 6.2. Current sizes recorded at pH_i = 6.2 without Ca^{2+} were divided by those at pH_i = 7.5 without Ca^{2+}. C. Macroscopic GV curves at pH_i = 7.5 (open circles) and pH_i = 6.2 (filled circles) without Ca^{2+}. The $V_{0.5}$ values for the two conditions were 161.1 ± 2.6 mV (8) and 102.6 ± 3.8 mV (8). The Q_{app} values were 1.22 ± 0.041 e_0 (8) and 1.33 ± 0.055 e_0 (8). D. The double mutants H365R:H394R and H365A:H394A are largely insensitive to changes in pH_i. GV curves with pH_i = 7.5 (open circles) and 6.2 (filled circles) in H365R:H394R (*left*) and in H365A:H394A (*right*). n=6 and 9 for the H365R:H394R and H365A:H394A, respectively. The $V_{0.5}$ values for the pH_i =7.5 and 6.2 data for the H365R:H394R channel were 109.6 ± 4.9 mV and 102.1 ± 3.3 mV and the Q_{app} values were 1.31 ± 0.07 e_0 and 1.30 ± 0.05 e_0. The respective values for the H365A:H394A channel were 177.7 ± 1.4 mV and 171.3 ± 1.7 mV, and 1.31 ± 0.03 e_0 and 1.30 ± 0.04 e_0. n = 6 and 9 for H365R:H394R and H365A:H394A, respectively.

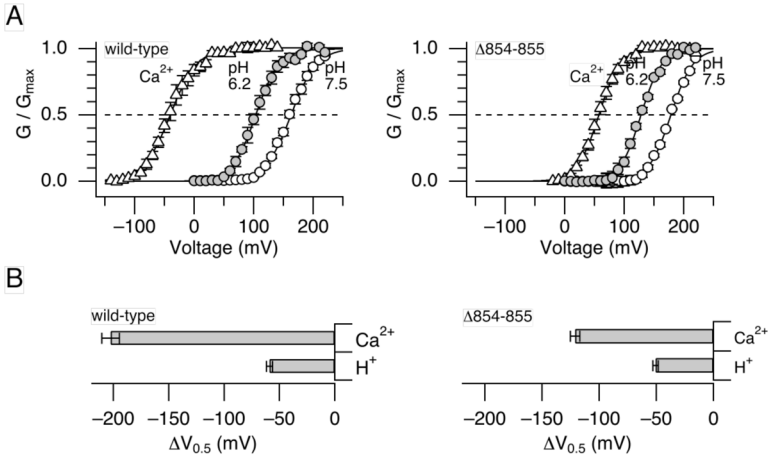

Figure 2.

Comparison of GV curves at high concentrations of Ca^{2+} and H^+. A. GV curves for the wild-type (*left*) and the Ca^{2+} bowl-defective (Δ854-846; *right*) Slo1 channels at pH_i = 7.5 without Ca^{2+} (open circles), at pH_i = 6.2 without Ca^{2+} (filled circles), and at pH_i = 7.2 with 200 μM Ca^{2+} (open triangles). B. Changes in $V_{0.5}$ by pH_i = 6.2 (designated as "H^+") and 200 μM Ca^{2+} ("Ca^{2+}") for the wild-type (*left*) and Δ854-846 (*right*) channels. n=5 and 9 for the wild-type and Δ854-846 channels, respectively.

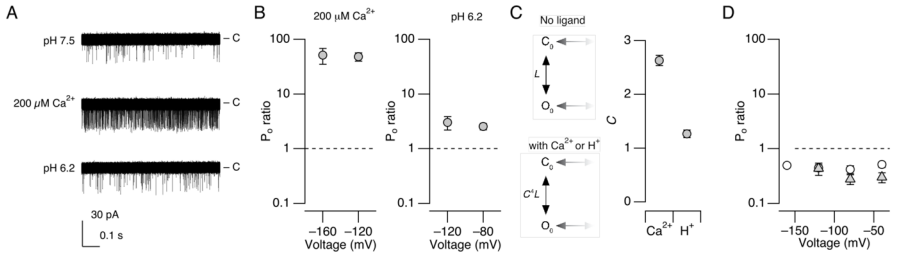

Figure 3.

Relative effects of Ca^{2+} and H^+ in enhancing P_o at negative voltages. A. Representative openings at −120 mV at pH_i = 7.5 without Ca^{2+} (*top*), pH_i = 7.5 with 200 μM Ca^{2+} (*middle*) and pH_i = 6.2 without Ca^{2+} (*bottom*) in the Ca^{2+} bowl-defective Slo1 mutant channel (Δ854-846). The patch contained ~85 channels. Sixty 1-s data segments are shown superimposed. The closed level is indicated by "c". B. Relative P_o with 200 μM Ca^{2+} at pH_i =7.5 (left) and pH_i = 6.2 without Ca^{2+} (right) compared with P_o at pH_i =7.5 without Ca^{2+} in the Slo1 Δ854-846 channel. P_o in each condition was normalized to that measured at pH_i = 7.5 without Ca^{2+} in each patch. C. Estimated value of the HA model parameter *C* for Ca^{2+} (200 μM) and H^+ (pH_i = 6.2) using the results obtained at −120 mV in the Slo1 Δ854-846 channel. The P_o ratio values were raised to the ¼th power to estimate *C*. The top diagram shows a subset of the HA model at negative voltages without any ligand and the bottom diagram shows the same subset with saturating Ca^{2+} or H^+. D. Relative P_o at pH_i = 6.2 without Ca^{2+} compared with P_o at pH_i =7.5 without Ca^{2+} in the H365R:H394R channel (open circles) and the H365A:H394A channel (filled triangles).

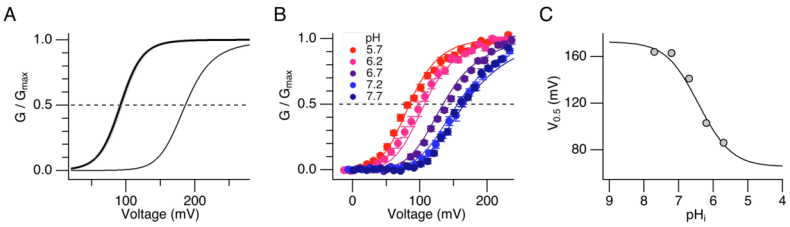

Figure 4.

GV curves simulated by the HA model with changes in the value of the coupling factor *C* for the Ca^{2+} bowl-defective Slo1 channel. A. Simulated GV curves for the conditions with no Ca^{2+} (thin curve) and with 200 μM Ca^{2+} (thick curve). The value of *C*, 2.6 ± 0.09, was estimated based on the P_o measurements at −120 mV. The line width of the GV curves represents SEM. B. GV results at different pH_i fit with the HA model (smooth curves) with $C = 2.14$ and $K_D = 1.31$ μM. The measured results are from Avdonin et al.[25] C. The $V_{0.5}$-pH_i relation from B is compared with the prediction of the model. The model accounts for an approximate − 50 mV GV shift from pH 7.5 to 6.2 while also predicting a 3.97-fold increase in P_o at −120 mV, similar to the observed 3.14-fold increase. Most of the other parameters in the model were fixed to values previously determined by Horrigan et al ($z_J = 0.55$ e_0, $z_L = 0.38$ e_0, $D = 11.6$, $E = 2.4$), while $L_0 = 7.1 \times 10^{-6}$ and $V_h(J) = 94$ mV were allowed to vary freely.

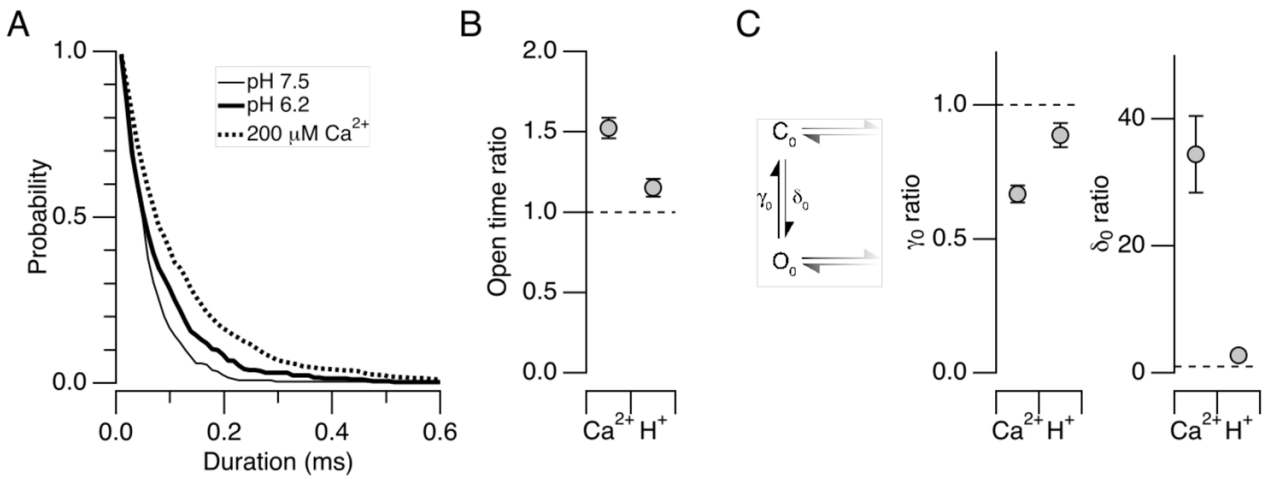

Figure 5.

Changes in the single-channel kinetics of the Ca^{2+} bowl-defective Slo1 Δ854-846 channel at −120 mV by Ca^{2+} and H^+. A. Representative open duration distributions at pH_i = 7.5 without Ca^{2+} (thin curve), at pH_i = 6.2 without Ca^{2+} (thick curve), and pH_i = 7.5 with 200 μM Ca^{2+}(dashed curve). Each curve shows the probability that the open dwell time is greater than the value indicated on the abscissa. B. Fractional changes in the mean open time by 200 μM Ca^{2+} or with H^+ at pH_i = 6.2 normalized with the control value at pH_i = 7.5 without Ca^{2+}. The mean open durations at pH_i = 7.5 without Ca^{2+}, pH_i = 6.2 without Ca^{2+}, and at pH_i = 7.5 with 200 μM Ca^{2+} were 0.77 ± 0.005 (13), 0.85 ± 0.003 (10), and 1.2 ± 0.01 (9) ms, respectively. C. Changes in the opening and closing rate constants γ and δ in the HA model. The diagram depicts the two states in the HA model operative at negative voltages where VSD activation is negligible. The value of γ_0 was estimated as the reciprocal of the mean open time and that of δ_0 was derived from P_o and γ_0 using the expression $P_o = \delta_0/(\delta_0 + \gamma_0)$. The rate constant values are normalized to the respective values recorded at pH_i = 7.5 without Ca^{2+} in each patch. The values of γ (s^{-1}) for the results obtained at pH_i = 7.5 without Ca^{2+}, pH_i = 6.2 without Ca^{2+} and at pH_i = 7.5 with 200 μM Ca^{2+} were 13, 342 ± 642 (13), 11, 858 ± 395 (10) and 9, 028 ± 586 (9), respectively. For δ, the values (s^{-1}) were 0.013 ± 0.002 (13), 0.025 ± 0.004 (10), and 0.35 ± 0.09 (9), respectively.

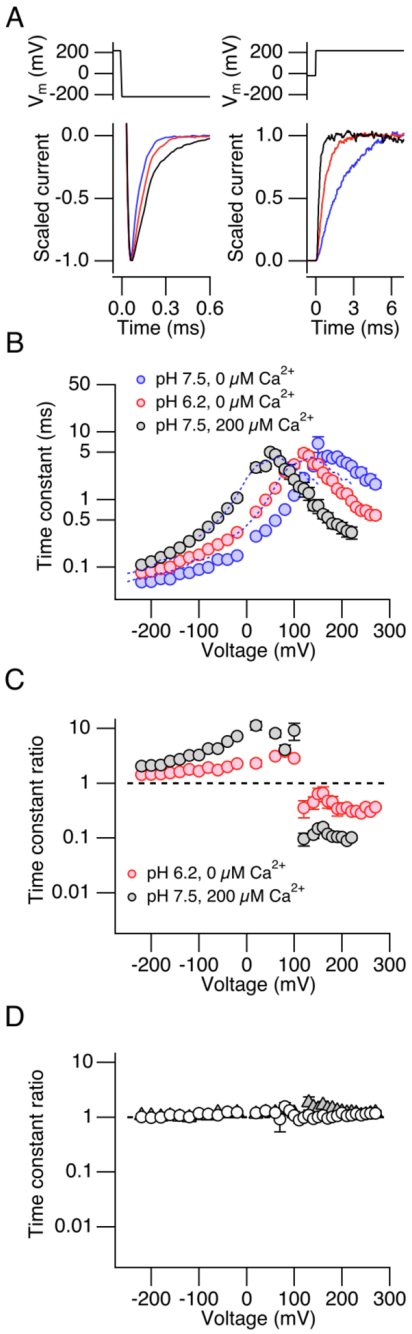

Figure 6.

Differential effects of high concentrations of H^+ and Ca^{2+} on the macroscopic kinetics of the Ca^{2+} bowl-defective mutant Slo1 Δ854-855. A. Representative scaled currents at −200 mV (*left* panel) and 220 mV (*right* panel) at pH_i = 7.5 (blue) or pH_i = 6.2 without Ca^{2+} (red), and pH_i =7.5 with 200 μM Ca^{2+} (black). B. Voltage dependence of the activation and deactivation time constant at pH_i = 7.5 (blue) or pH_i = 6.2 without Ca^{2+} (red) and pH_i =7.5 with 200 μM Ca^{2+} (black) in the Slo1 Δ894-895 channel. n=10. C. Fractional changes in the activation and deactivation time constant on decreasing pH_i from 7.5 to 6.2 without Ca^{2+} (red) or increasing $[Ca^{2+}]_i$ to 200 μM at pH_i = 7.5 (black). The time constant values were normalized to those measured at pH_i = 7.5 without Ca^{2+} in each patch. n=10. D. Fractional changes in the activation

and deactivation time constant by low pH_i = 6.2 in the H365R:H394R (open circles) and H365A:H394A channels (filled triangles). At ≤100 mV, the values for the two mutants are very similar and the triangles are not discernible. $n \geq 6$.

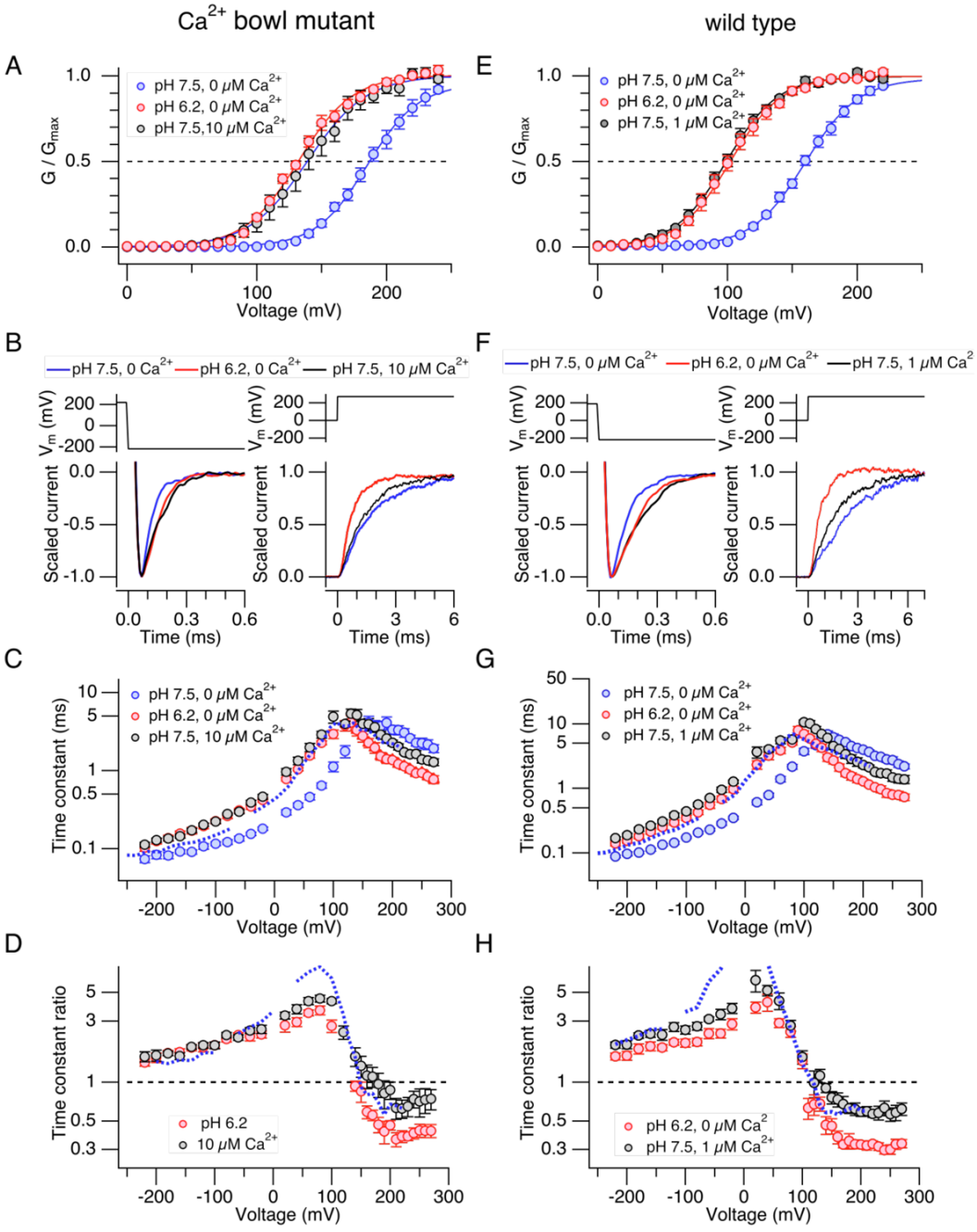

Figure 7.

Titration of the steady-state activation of the Ca^{2+} bowl-defective Slo1 mutant (Δ854-855; A–D) and of the wild-type channel (E–F) with Ca^{2+} and H^+. A, E. Macroscopic GV curves at pH_i = 7.5 without Ca^{2+} (blue), pH_i = 6.2 without Ca^{2+} (red) and pH_i = 7.5 with 10 μM Ca^{2+} (black) in the Ca^{2+} bowl-mutant channel (A) and with 1 μM Ca^{2+} (black) in the wild-type channel (E). The $V_{0.5}$ values for the three conditions in the Ca^{2+} bowl mutant were 188.8 ± 3.6 mV (6), 132.2 ± 2.1 mV (6) and 139.5 ± 7.3 mV (6), respectively, and those for the wild-type channel were 161.1 ± 2.6 mV (8), 102.6 ± 3.8 mV (8) and 99.5 ± 3.0 mV (8), respectively. The Q_{app} values were for the Ca^{2+} bowl mutant were 1.23 ± 0.067 e_0 (6), 1.34 ± 0.072 e_0 (6) and 1.27 ± 0.073 e_0 (6), and those for the wild-type channel were 1.22 ± 0.041 e_0 (8), 1.33 ±

0.055 e_0 (8) and 1.28 ± 0.042 e_0 (8). B, F. Representative scaled currents at −220 mV (*left*) and 270 mV (*right*) in response to the voltage pulses shown (*top* in each panel) in the Ca^{2+} bowl mutant (B) and the wild-type channel (F). C, G. Voltage dependence of the activation and deactivation time constant in the Ca^{2+} bowl mutant (C) and the wild-type channel (G). The dashed blue curve shows the results at pH_i = 7.5 without Ca^{2+} shifted by −58 mV in C and −60 mV in G. n= 6 and 8. D, H. Fractional changes in the activation and deactivation time constant by pH_i = 6.2 without Ca^{2+} (red) and pH_i = 7.5 with 10 μM Ca^{2+} (black) in the Ca^{2+} bowl-mutant channel (D) and 1 μM Ca^{2+} (black) in the wild-type channel (H). The dashed blue curve shows the results expected from shifting the time constants measured at pH_i = 7.5 without Ca^{2+} by −50 mV in (D) and −60 mV in (G).

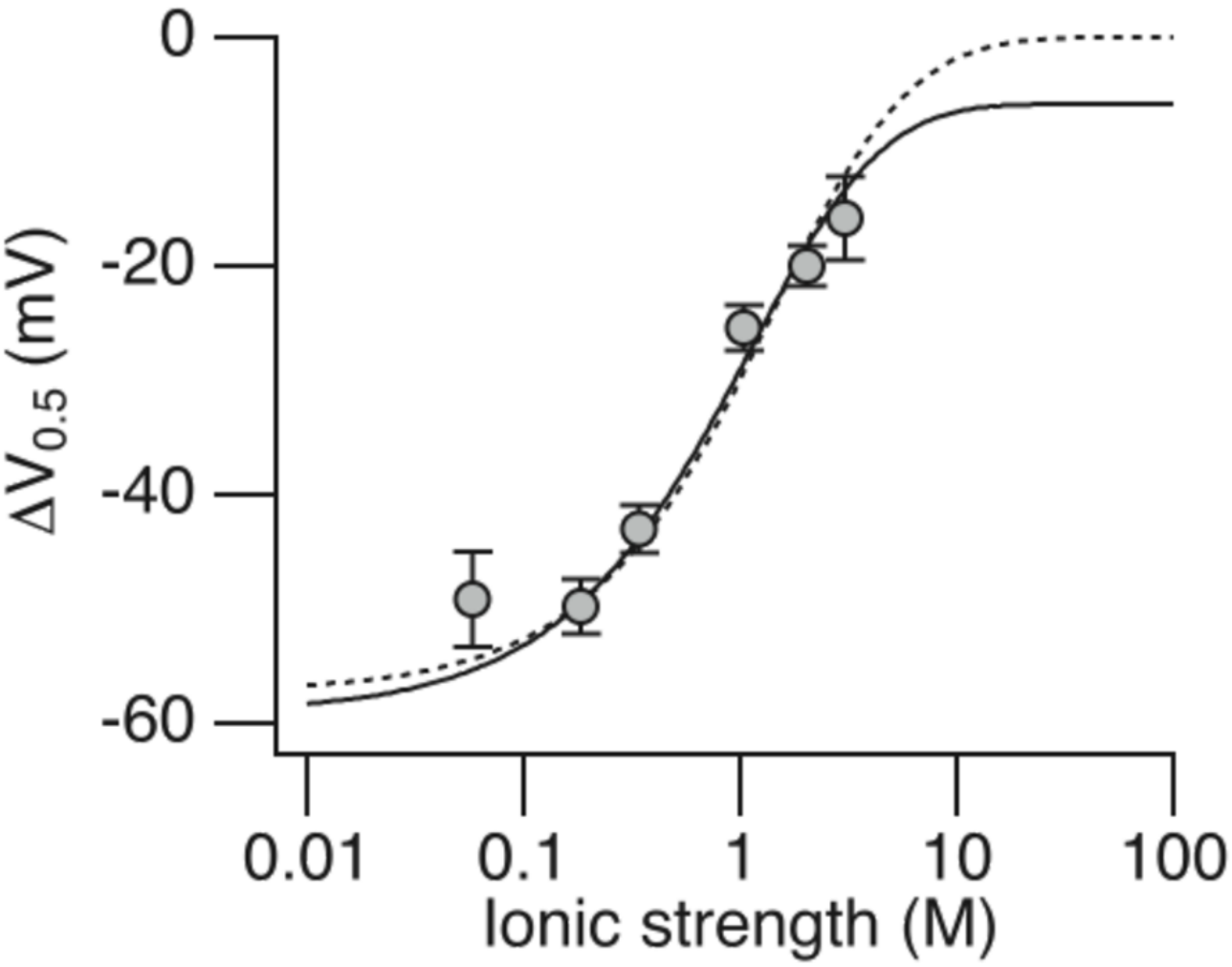

Figure 8.

Fit of the dependence of $V_{0.5}$ on ionic strength using the Debye-Hückel formulation together with the HA model. ΔV0.5 was measure from pH_i 7.2 to 6.2 for the wild-type channel in different concentrations of KCl (from Hou et al. 22). Model parameters at ionic strength 0.18 M were determined from Fig. 4 (z_J = 0.55 e_0, $V_h(J)$ = 94 mV, $L_0 = 7.1 \times 10^{-6}$, z_L = 0.38 e_0, K_D = 1.31 μM, *C* = 2.14, *D* = 11.6, *E* = 2.4). The solid fit was obtained with the assumption that *C* varies with ionic strength according to the Debye-Hückel formulation (see text for details), while *E* remains constant (R_C = 8.8 ± 0.7 Å and R_O = 5.4 ± 0.5 Å). The dashed fit assumed that both *C* and *E* vary with ionic strength (R_C = 5.7 ± 0.3 Å and R_O = 4.2 ± 0.2 Å). For simplicity, the two His residues in the RCK1 sensor were assumed to interact with a negative charge in the resting VSD at a distance (R_R), which was set equal to R_C. The dashed fit predicts a decrease in this distance with voltage-sensor activation of 1.6 Å.